ADVANCING EARTH AND SPACE SCIENCES

Geophysical Research Letters

RESEARCH LETTER
10.1029/2023GL107301

On the Role of Indian Ocean SST in Influencing the Differences in Atmospheric Variability Between 2020–2021 and 2021–2022 La Niña Boreal Winters

Tao Zhang[1,2] **and Arun Kumar**[2]

[1]ESSIC, University of Maryland, College Park, MD, USA, [2]NOAA/NCEP/Climate Prediction Center, College Park, MD, USA

Key Points:

- The difference in observed atmospheric anomalies for 2022 versus 2021 La Niña boreal winters featured a Northern Hemisphere tripole pattern
- Indian Ocean SST contributed to the formation of observed tripole pattern, with internal atmospheric variability modulating its magnitude
- Errors in SST predictions over the Indian Ocean led to the failure in predictions of the circulation changes in NMME forecasts

Supporting Information:

Supporting Information may be found in the online version of this article.

Correspondence to:

T. Zhang,
tao.zhang@noaa.gov

Citation:

Zhang, T., & Kumar, A. (2024). On the role of Indian Ocean SST in influencing the differences in atmospheric variability between 2020–2021 and 2021–2022 La Niña boreal winters. *Geophysical Research Letters*, *51*, e2023GL107301. https://doi.org/10.1029/2023GL107301

Received 14 NOV 2023
Accepted 25 FEB 2024

Abstract The difference in observed atmospheric anomalies over the Northern Hemisphere winter between 2021–22 and 2020–21 La Niña years indicated a tripole pattern consisting of a Japan cyclone, a Bering Sea anticyclone, and a cyclone over the North American continent. This feature, however, was not replicated in the North American Multi-Model Ensemble (NMME) forecasts. A set of model sensitivity experiments was performed to better understand the cause of this discrepancy. The results revealed the possible role of the influence of sea surface temperature (SST) anomalies, particularly over the Indian Ocean, on the observed circulation differences that was further modulated by internal atmospheric variability. The failure in predicting circulation changes in NMME was next attributed to the errors in SST predictions over the Indian Ocean and highlights the need for improvements in SST forecasts over this region.

Plain Language Summary The tropical SST anomalies associated with the El Niño-Southern Oscillation (ENSO) are known to influence the global atmospheric circulation and are the major source of skill in U.S. seasonal predictions. As the cold phase of ENSO, La Niña features below-normal SST anomalies and suppressed convection over the equatorial central and eastern Pacific. Such a tropical heating distribution favors the formation of the atmospheric circulation pattern that has a roughly opposite effect on U.S. surface climate compared to El Niño, the warm phase of ENSO, although the effect is not strictly symmetric. For the recent two La Niña boreal winters of 2020–21 and 2021–22, the observed circulation patterns differed, but dynamical seasonal prediction failed to replicate this feature. Understanding the cause for the discrepancy of circulation changes between prediction and observations is of fundamental importance for the improvement of seasonal forecasts. Toward this, we designed numerical experiments that are forced with observed and predicted SST anomalies over different ocean basins. The results show that it is the errors in SST prediction over the Indian Ocean that contributed to the failure in the prediction of circulation changes, highlighting the importance of skillful prediction of SST over this region.

1. Introduction

2020-2022 boreal winters were a continuation of La Niña, with 2020/21 years being a moderate La Niña event and 2021/22 a comparable La Niña event (Cao et al., 2022; Li et al., 2022, 2023). For these two consecutive La Niña winters, sea surface temperatures (SSTs) in 2021/22 relative to 2020/21 were warmer over the central North Pacific, the North Atlantic, the Indian Ocean and the equatorial central Pacific, and were colder over the equatorial eastern Pacific (Figure 1, bottom left). The observed precipitation difference exhibited a pattern of dryness over 15°S–15°N and wetness south of 15°S over the central Indian Ocean and a wet condition over the maritime continent and near the Intertropical Convergence Zone (ITCZ).

There were also large differences in the observed heights located in the Northern Hemisphere with a tripole pattern consisting of cyclonic anomalies over Japan, anticyclonic anomalies over the Bering Sea, and cyclonic anomalies over the North American continent (Figure 1, bottom right), consistent with previous findings that multiyear La Niña could have different impacts over the North Pacific on different years, featuring enhanced atmospheric circulations anomalies over the North Pacific in second cold seasons compared to first cold seasons of La Niña based on composite analysis (Nishihira & Sugimoto, 2022; Okumura et al., 2017). The observed extratropical atmospheric anomalies can be influenced by the atmospheric internal variability (Kumar & Hoerling, 1995; Zhang et al., 2014), extratropical SST forcing (Beaudin et al., 2023) and SST anomalies in the tropical Indian and Pacific Ocean basins (Annamalai et al., 2007; Hoerling & Kumar, 2002). A question is

10.1029/2023GL107301

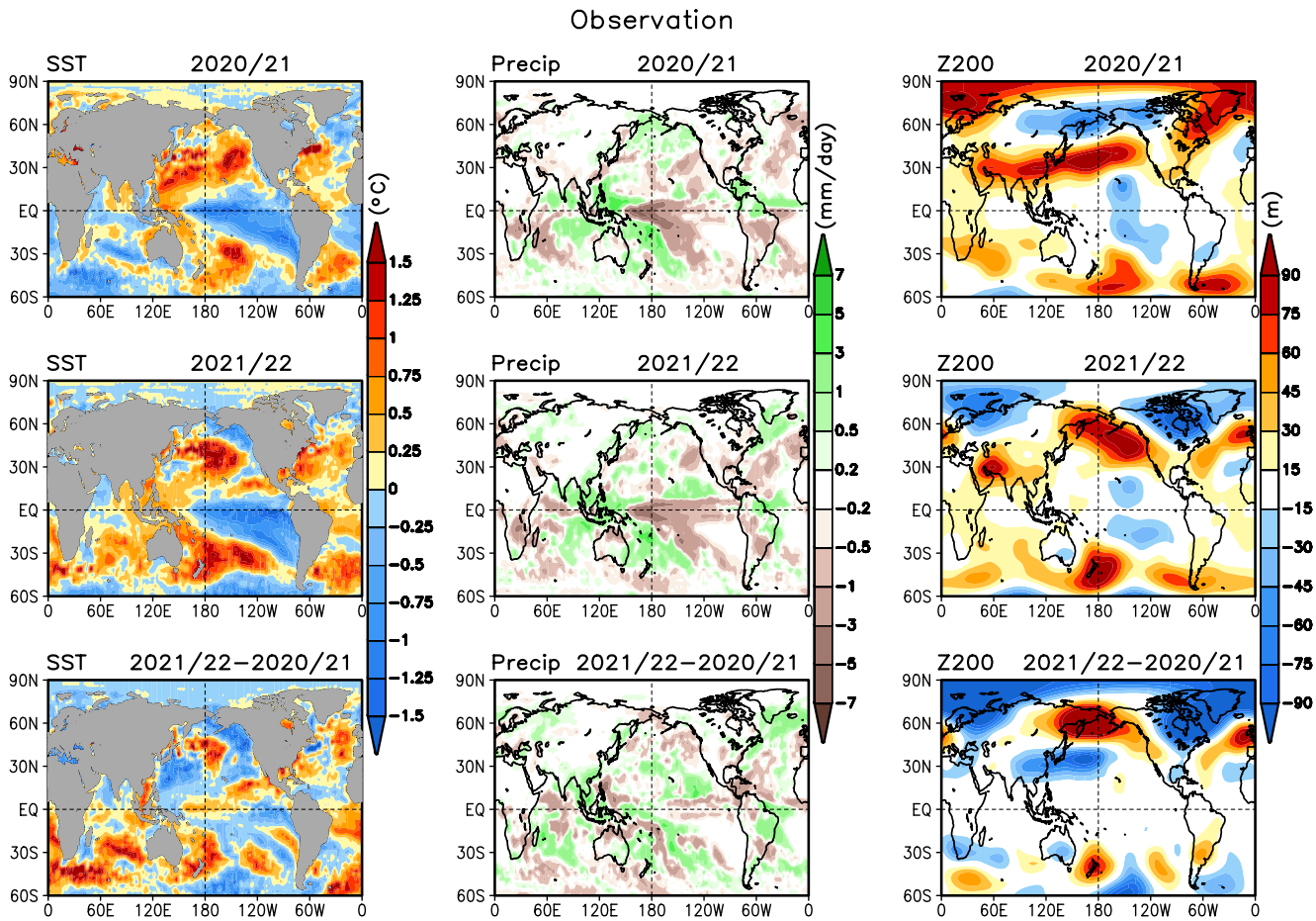

Figure 1. Observed November-March averaged (left) SST anomalies, (center) precipitation anomalies, and (right) 200-hPa height anomalies for (top) 2020/21 and (middle) 2021/22 and (bottom) their difference.

posed as to what component of the observed tripole pattern of the height difference between two La Niña events was due to atmospheric internal variability and what was a consequence of differences in the atmospheric response to the change in SSTs in different ocean basins. The latter possibility is especially pertinent as the wave train structure of tripole pattern in the observed height difference suggests its origin to be associated with rainfall (i.e., heating) anomalies in the vicinity of the eastern Indian Ocean and the Maritime continent.

The North American Multi-Model Ensemble (NMME) (Kirtman et al., 2014) prediction system currently provides real-time seasonal predictions that are used as a guidance by NOAA Climate Prediction Center (CPC) operational seasonal forecasters. In contrast to observations, however, NMME ensemble mean forecasts predicted a difference in height that was much smaller (Figure 2). Although the difference in the amplitude between model predicted and observed heights could be due to a comparison between ensemble mean (for the NMME prediction) and individual instances of seasonal means (in observations), an important point to note is that even the sign of difference in predicted height anomaly over the Pacific/North American (PNA) region differed from that for observations. Further, differences in SST predictions for these two years were found to be unlike the corresponding observed differences, particularly over the eastern Indian Ocean and maritime continent where the predicted SST difference was colder and the predicted precipitation difference was drier. It is noted that while the differences in the observed SST anomalies in these two winters were qualitatively well predicted in the North Pacific, the South Pacific and most of the Atlantic Ocean, the forecast of SST difference between two winters had an opposite sign to observations in the vicinity of eastern Australia and the eastern equatorial Pacific because the NMME prediction missed the stronger warming and cooling in the winter of 2021/22 over these two regions, respectively.

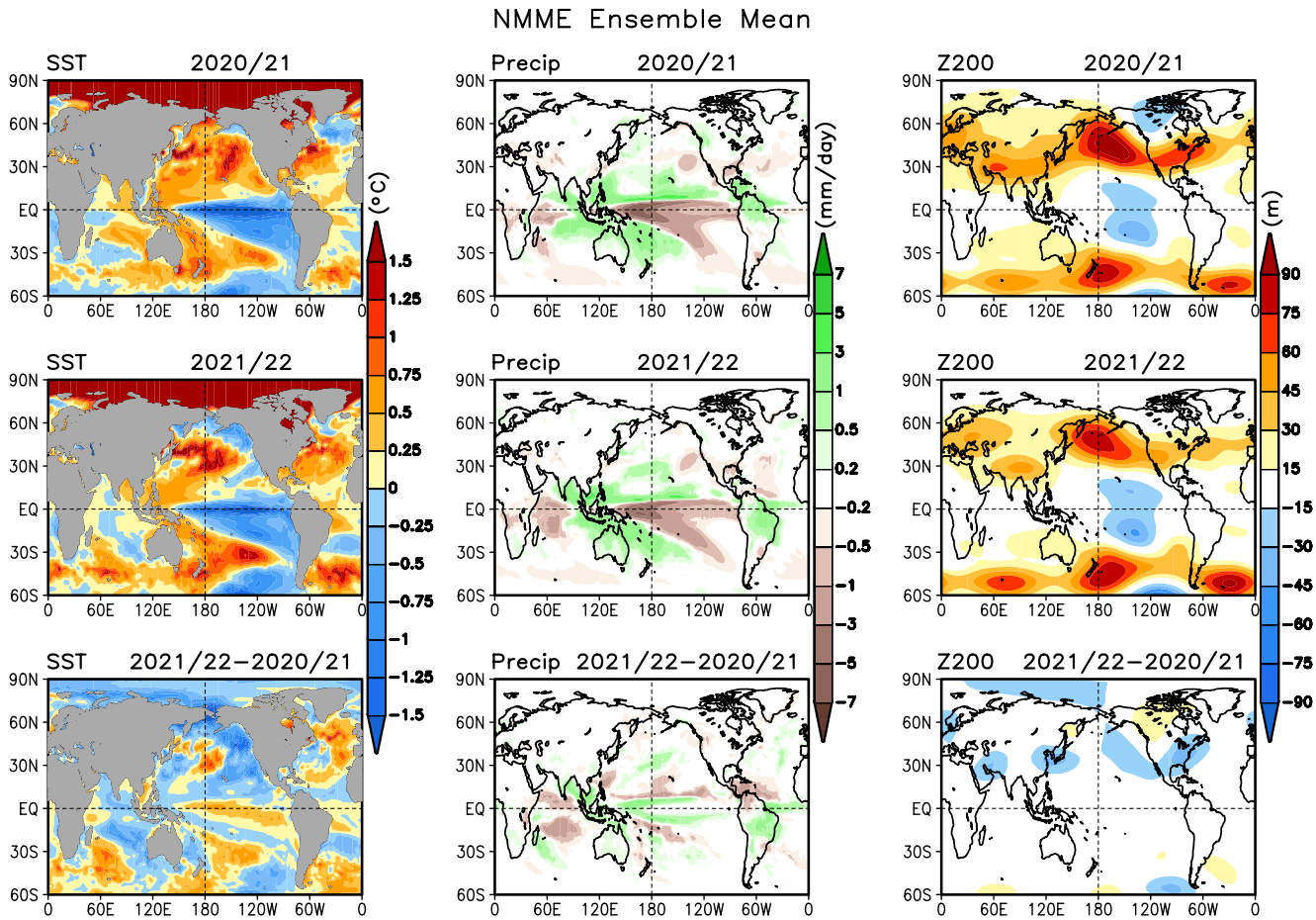

Figure 2. Ensemble-mean NMME predictions of November-March averaged (left) SST anomalies, (center) precipitation anomalies, and (right) 200-hPa height anomalies for (top) 2020/21 and (middle) 2021/22 and (bottom) their difference based on November initialization from 6 models.

Previous studies have shown that other than the tropical Pacific, the tropical Indian Ocean is also a possible region for the excitation of tropical-extratropical teleconnections (Annamalai et al., 2007; Bader & Latif, 2005; Hoerling et al., 2004; Hu et al., 2023; Kumar et al., 2010). Was it the error in predicted SST in NMME that led to the difference in sign for the height forecasts? This possibility is indicated by the results of Kumar et al. (2010) who found that the SST in the Indian Ocean and western Pacific warm pool region plays an important role in the attribution of the atmospheric teleconnections during La Niña events and is the question that is explored further in this analysis.

The focus and the motivation of this study is to design atmospheric general circulation model (AGCM) simulations in order to better understand (a) the differences in atmospheric responses to observed differences in SSTs, (b) role of SST errors in the NMME forecast over the Indian Ocean in misrepresenting atmospheric anomaly differences, and (c) causality of differences in observed atmospheric anomalies by exploring the role of the observed SSTs and internal atmospheric variability. In the analysis approach followed in the paper we would like to emphasize that (a) the intent is to understand the causality of differences in height response over two winters, (b) by analyzing the differences the possible issue of influence of biases in the mean state on tropical-extratropical interactions is circumvented, and (c) analysis of difference, by removing the dominant influence of La Niña on the atmospheric response, brings the secondary influence of SST anomalies in other ocean basins to the fore.

The paper is structured as follows. Section 2 describes the observational and NMME datasets as well as the model experiments. Section 3 first presents the differences in atmospheric responses between two La Niña years in Atmospheric Model Intercomparison Project (AMIP) simulations, and then using sensitivity experiments, the role

of the observed SST difference over various ocean basins is explored. Finally, sensitivity in the atmospheric response to errors in NMME SST forecast is assessed. Conclusions and discussions are given in Section 4.

2. Data and Model Simulations

The observed upper-level circulation patterns are analyzed based on 200-hPa geopotential height fields from the National Centers for Environmental Prediction (NCEP)–National Center for Atmospheric Research (NCAR) reanalysis (Kalnay et al., 1996). The observed global precipitation is from the Global Precipitation Climatology Project (GPCP) data set (Huffman et al., 1997), and the observed SSTs are from the Hurrell data set (Hurrell et al., 2008).

To evaluate the NMME predicted atmospheric response, we consider the grand ensemble mean forecasts (the total ensemble size is 87) that include a total of six NMME models: CanCM4i, NCEP_CFSv2, GEM_NEMO, GFDL_SPEAR, NCAR_CCSM4 and NASA_GEOS5v2. For each month, the NMME models are initialized on the first day of the month and produce 9-month-long forecasts. We utilize the forecasts at 0-month lead that are initialized in November and predict the subsequent 5-month average of November–March for 2021 and 2022 La Niña events. An analysis for 5-month average is used to cover the boreal cold season to enhance the signal-to-noise ratio.

Because of the small number of La Niña events and possible role of internal atmospheric variability in observations, we examine the response to observed SST difference between two La Niña events using large ensembles of AMIP simulations, to separate forced signals from the atmospheric internal variability. The 100-member ensemble is based on FV3GFS (Zhou et al., 2019), which realistically simulates the observed climate variability and trends, as well as the observed features associated with the atmospheric response to ENSO. Running at C96 horizontal resolution (about 100 km) and 64 vertical levels, FV3GFS model is forced with specified boundary conditions that include observed monthly varying SSTs, sea ice (Hurrell et al., 2008), and carbon dioxide concentrations for 1979–2022. Other greenhouse gases, aerosols, and solar forcings etc. are specified with climatological values in the model. Anomalies are calculated relative to a 1991–2020 reference period for AMIP simulations, observations, and NMME data.

Additional atmospheric model simulations based on FV3GFS are designed to better understand the relative contributions of observed SST difference between two years from various ocean basins and to assess the impacts of errors in the NMME predicted differences in SST. For the sensitivity experiments, a 40-year control experiment using repeating seasonal cycle of observed climatological SST boundary forcings based on a 1991–2020 mean is first completed. Four perturbation experiments, also of 40-year duration, are conducted in which SST change increments (November 2021–March 2022 averages minus November 2020–March 2021 averages) are added to the observed climatological SSTs of the control run, while all other forcings are unchanged. Note that the increment is based on the November–March change, and that same increment is added to November–March of 5-calendar months with a linear tapering in other 7-calendar months.

The SST increment for the first perturbation experiment is based on the observed SST change over the globe, and that for the second perturbation experiment is based on the observed SST change over the tropics (30°S–30°N). The increment for the third and fourth perturbation experiments is based on the observed and NMME predicted SST change over the Indian Ocean region (30°S–30°N, 30°E–140°E), respectively. As all experiments utilize identical sea ice concentration, greenhouse gas and aerosol concentrations, these simulations isolate the sensitivity to changes in SST patterns.

3. Results

3.1. Atmospheric Response in AMIP Simulations

To explore the possible cause for the observed tripole pattern of height difference between two La Niña winters, we employ the AMIP ensemble to assess differences in atmospheric response between two winters. In response to differences in SSTs (Figure 1 bottom left), precipitation differences in the FV3GFS AMIP simulations between two La Niña winters are characterized by a wet condition over the southern Indian Ocean, maritime continent and ITCZ region (Figure 3 bottom left). Of particular relevance is the correspondence between wet conditions over the southern Indian Ocean and warmer SSTs underneath with the latter acting as a forcing for the rainfall.

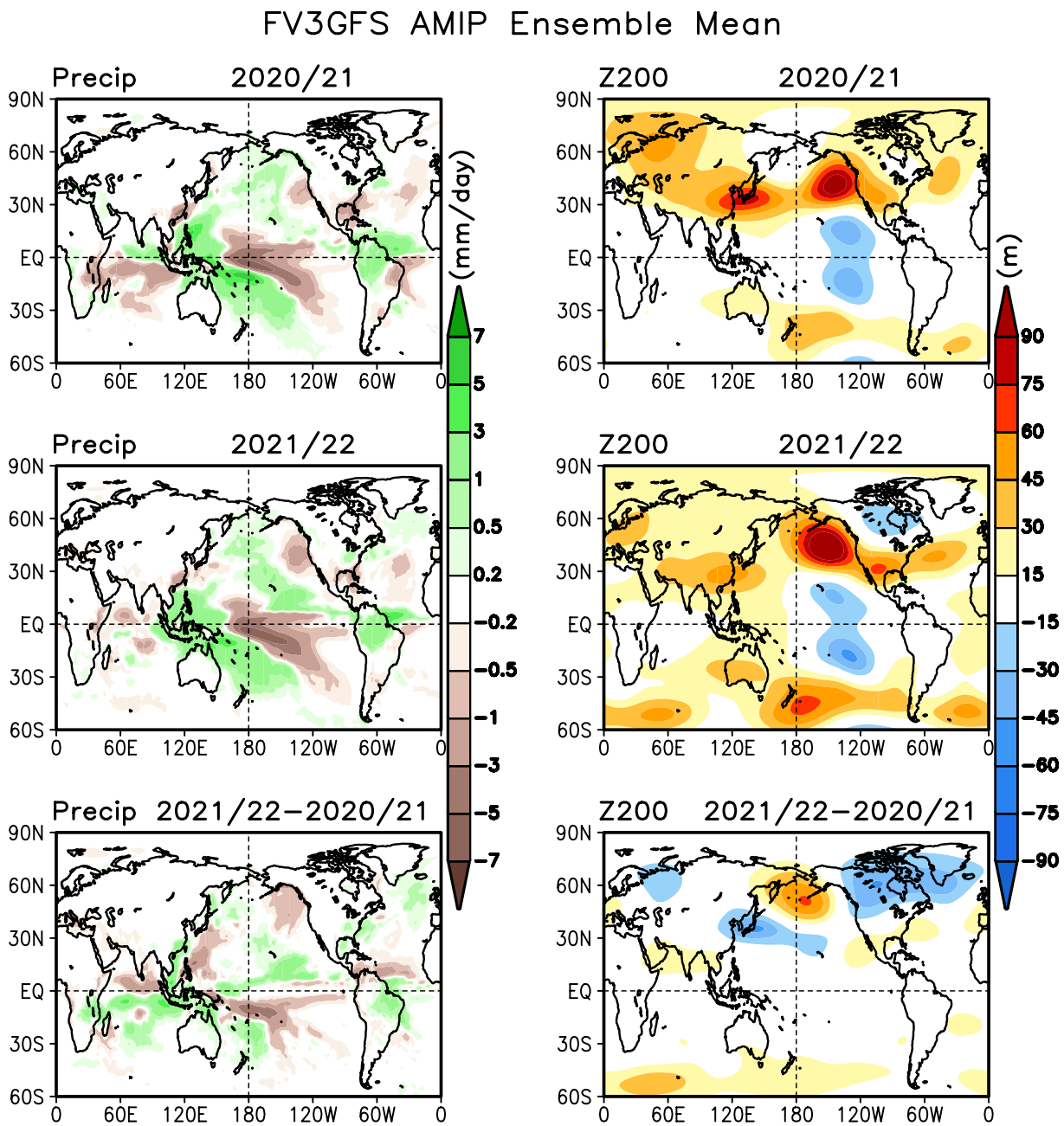

Figure 3. FV3GFS simulated 100-member ensemble mean November-March averaged (left) precipitation anomalies and (right) 200-hPa height anomalies for (top) 2020/21 and (middle) 2021/22 and (bottom) their difference. Precipitation and circulation shaded values are statistically significant at the 95% confidence level with the *t* test.

AMIP ensemble mean results show that although 200-hPa height anomalies for both years largely follow the La Niña composite pattern of atmospheric teleconnections (Zhang et al., 2014), differences between atmospheric responses have a weaker anticyclone over Japan, a northward shift of anticyclone over the North Pacific and a stronger cyclone over the North American continent in 2022 relative to 2021. These differences are similar to the observed counterpart (cf. right panels of Figures 3 and 1) with a spatial correlation of 0.61 over the extratropical Northern Hemisphere. For the AMIP simulations the SSTs are the *forcing* for the height difference pattern, raising the possibility for the same mechanism in observations.

In the comparison of difference between the ensemble mean of heights from AMIP simulations and observations it is important to keep in mind that while the former highlights the change in the atmospheric *response* to changes

in SSTs, the latter, in addition, could also be influenced by the atmospheric internal variability. In fact, this is the likely reason that the amplitude of changes in the model simulated atmospheric response is smaller than the observed anomalies.

To explore the role of internal atmospheric variability in shaping the observed anomalies, we also calculated the correlation between Northern Hemisphere 200-hPa height change pattern for observations and that simulated by the model based on the large sample size of differences between individual members in the ensemble (Figure S1 in Supporting Information S1). This approach results in a sample of 10,000 correlations with variability among different estimates coming from the internal variability in the difference in heights between pairs of atmospheric simulations taken from 2020 to 21 and 2021 to 22 winters. The range of 200-hPa height change pattern correlation has a scatter with values ranging from −0.71 to 0.85, and further, the distribution of correlation has a positive skew. Another important point to note is that the spatial pattern of the observed difference in 200-hPa heights is well within the range of possibilities indicated by the AMIP simulations, and therefore, is a plausible outcome consistent with changes in SSTs.

To further illustrate this point, we make composites for the four samples that had the best or the worst correlation among the large model sample differences (Figure S2 in Supporting Information S1), following the procedure of Kumar et al. (2013). The analysis indicates that the observed 200-hPa height change over the Northern Hemisphere is well replicated from the composite of the best four samples, with a spatial correlation of 0.91 and a comparable magnitude as indicated by the similarity in the root mean square values of anomalies. The analysis also indicates that at the same time the possibility also exists that model simulated difference could have been opposite to the observed difference, however, the skewness of the frequency distribution would argue that its probability of occurrence for that would be lower. To illustrate this, we also show the composite of four samples that have the largest negative correlation of 200-hPa height change with the observation.

The results indicate that despite the apparent influence of SST on the observed height change, the internal atmospheric variability could also have played a role in determining the magnitude discrepancy between difference in the ensemble mean response to changes in SSTs and the corresponding change in the observation (i.e., equivalent to individual model simulation). From this analysis it is clear that the FV3GFS simulations can realistically reproduce the observed 200-hPa height change.

3.2. Atmospheric Response to Observed SST Forcing in Sensitivity Experiments

The above analysis shows that an SST forced change is evident in the Northern Hemisphere 200-hPa teleconnection response between 2022 and 2021 La Niña events. To identify in which ocean basin SST changes are responsible for the atmospheric circulation changes, a set of additional idealized AGCM simulations with observed SST differences between 2022 and 2021 La Niña years (Figure 1, bottom left) is conducted. For each sensitivity experiment, the specified SST anomalies over various ocean basins were superimposed on the climatological SST used in the control experiment (see Section 2 for details). Both sensitivity experiments and control experiments were run for 40 years and the results are shown as an average anomaly of November-March relative to the control simulation.

The responses of precipitation and 200-hPa height in three experiments are shown in Figure 4. Figure 4 (top center and right) is forced by the observed global SST pattern (top left), Figure 4 (middle center and right) is forced by observed tropical SST between 30°S and 30°N alone (middle left), and Figure 4 (bottom center and right) is forced by observed SST in the Indian Ocean (30°S–30°N, 30°E–140°E) alone (bottom left). The comparison between Figures 4 and 3 (bottom panel) shows that all idealized simulations have a similar precipitation response to the AMIP simulations. Specifically, these three experiments capture the prevalence of the wet condition over the southern Indian Ocean, maritime continent and ITCZ region and the dry condition over the northern Indian Ocean, the Philippine Sea, and the South Pacific Convergence Zone (SPCZ), except that the magnitude of precipitation response over the ITCZ region is somewhat weaker in the Indian Ocean alone simulation.

Given that the responses of tropical precipitation, which constitute the primary forcing for the atmospheric teleconnections, are almost identical in the idealized simulation (Figure 4, center column) and AMIP simulations (Figure 3, bottom row), it is not surprising that the height response patterns are also similar. More importantly, the Indian Ocean alone simulation closely reproduces the Northern Hemisphere height patterns that are also present in the global and tropics-alone experiments. The observed and the AMIP simulated tripole pattern of height

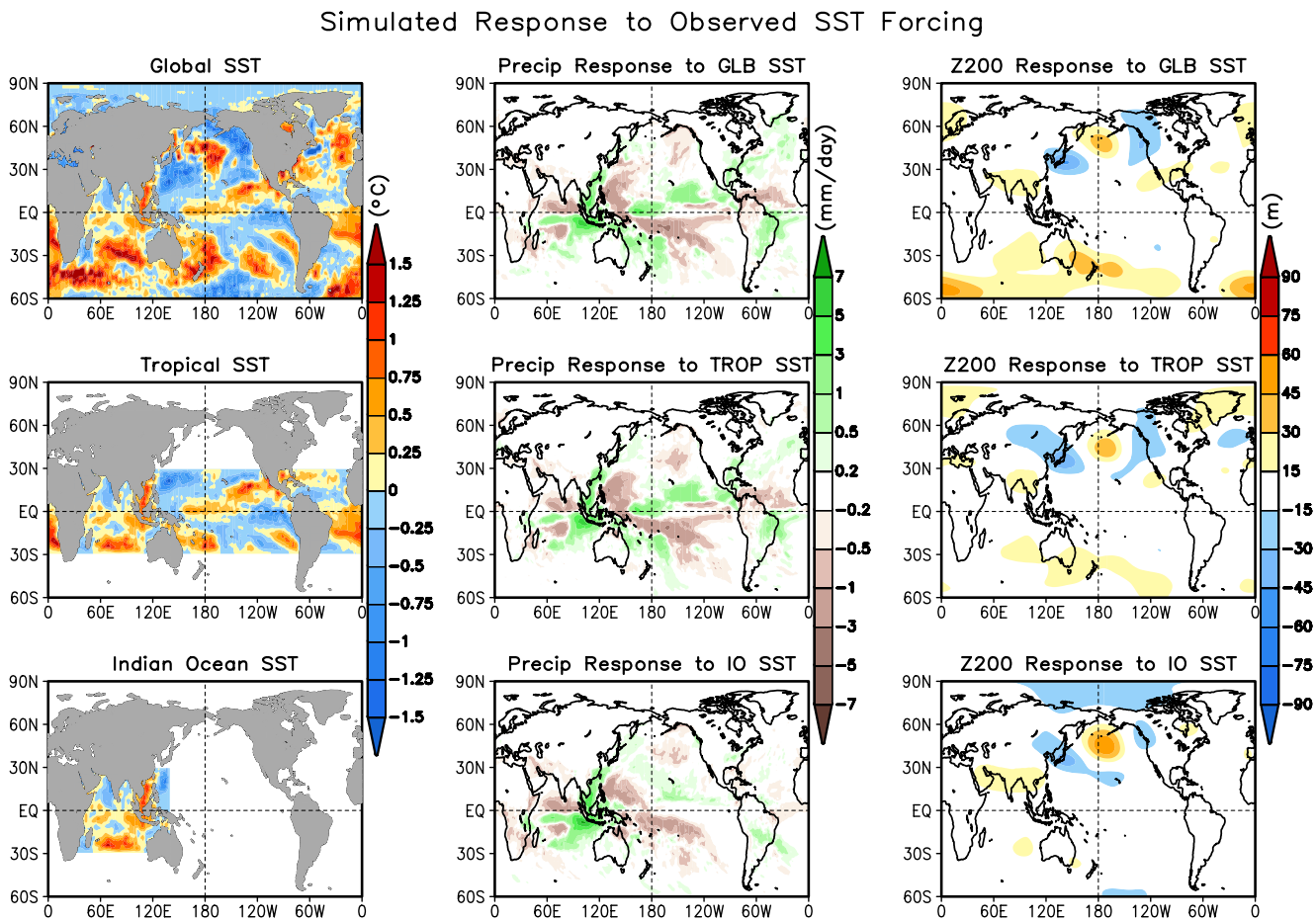

Figure 4. FV3GFS simulated responses of November–March averaged (center) precipitation and (right) 200-hPa height to (left) the observed SST forcings over (top) the global oceans, (middle) the tropical oceans, and (bottom) the Indian Ocean. The observed SST forcings are increments of November-March changes computed for (2021–2022) versus (2020–2021). Precipitation and circulation shaded values are statistically significant at the 95% confidence level with the *t* test.

change, therefore, can be captured by a model forced just by the SST anomalies in the Indian Ocean region, highlighting the important role of Indian Ocean SST in determining the differences in the atmospheric response to SSTs (Figure 3 bottom right).

3.3. Atmospheric Response to NMME SST Forcing in Sensitivity Experiments

To further understand the role of Indian Ocean SST in the atmospheric teleconnections and explore whether errors in the predicted Indian Ocean SST caused the failure in the predicted change in height response between two years in NMME, we performed the fourth idealized simulation forced with NMME predicted SST differences between 2022 and 2021 La Niña years over the Indian Ocean (30°S–30°N, 30°E–140°E) alone (Figure 5 top).

Consistent with the predicted SST difference that is largely opposite to the observation over the Indian Ocean, the precipitation response in the NMME Indian Ocean alone simulation is also opposite to that in the Indian Ocean alone simulation forced with observed SST difference, particularly over the eastern Indian Ocean, maritime continent and SPCZ region (cf. Figure 5 middle and Figure 4 bottom). The precipitation anomaly also does not render the formation of a tripole pattern of height response as noted in the Indian Ocean alone simulation forced with observed SST difference, instead, generates a North Pacific cyclone resembling the NMME predicted height change to some extent (cf. Figure 5 bottom and Figure 2 bottom right). The results indicate that the failure of the NMME predicted height change between 2022 and 2021 La Niña years to mimic observed anomalies could be due to the errors in predicted SSTs over the Indian Ocean. This argument is supported by additional Indian Ocean experiments in which SST forcing over the far tropical northwestern Pacific (TNWP) where the diabatic heating

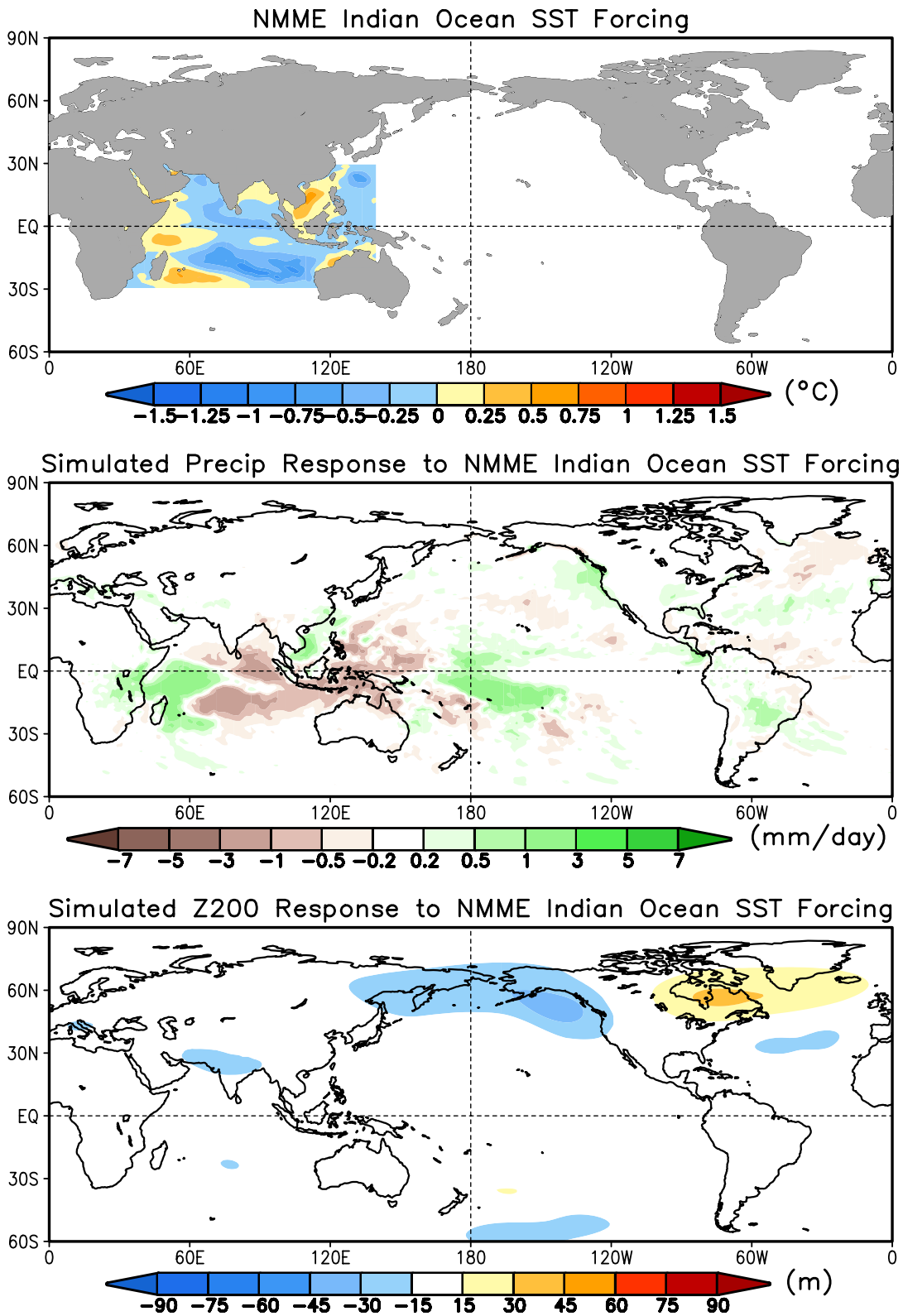

Figure 5. FV3GFS simulated responses of November–March averaged (middle) precipitation and (bottom) 200-hPa height to (top) NMME SST forcings over the Indian Ocean. The NMME SST forcings are increments of November-March changes computed for (2021–2022) versus (2020–2021) from NMME ensemble mean predictions based on November initialization from 6 models. Precipitation and circulation shaded values are statistically significant at the 95% confidence level with the *t* test.

could also contribute to atmospheric patterns over the North Pacific (Nishihira & Sugimoto, 2022), is excluded (Figure S3 in Supporting Information S1).

4. Summary and Discussion

Motivated by the observational evidence that the height *differences* between 2021–22 and 2020–21 La Niña years exhibited a tripole pattern over the Northern Hemisphere comprising a cyclone over Japan, an anticyclone over the Bering Sea, and a cyclone over the North American continent, and by the fact that NMME forecasts failed to capture the sign of the observed feature, AGCM model simulations were conducted to probe the role of SST in the height response over two La Niña winters.

The comparison between AMIP simulations and observations suggested that the ensemble mean response in height changes (due to changes in SSTs) had a moderately positive pattern correlation with observations, but the simulated magnitude was weaker. Further analysis revealed that while the SST effect on the formation of observed tripole pattern was evident, the magnitude difference of model ensemble mean from observations could be attributed to the atmospheric internal variability. In other words, while the change in the ensemble mean response across two winters was the expected (and potentially predictable) outcome, the difference from the observed heights can have added contribution from the atmospheric internal variability.

Additional sensitivity experiments forced with various regional SST anomalies demonstrated that the SST anomalies in the Indian Ocean were important in modulating the atmospheric teleconnections and the failure of NMME to even predict the sign of height changes could be attributed to the errors in predicted SST over the Indian Ocean. The results highlight the role of SST variability and its skillful prediction in the Indian Ocean, which could be an important area for seeking further improvements in seasonal forecasts.

The mechanism responsible for the formation of observed tripole pattern of height change is the differential SST warming in the Indian Ocean exciting a teleconnection pattern associated with Rossby wave propagation from the tropical Indian Ocean to the North American Continent via East Asia and the North Pacific, consistent with the results of Hu et al. (2023) who found a similar teleconnection associated with the modulation of tropical Indian Ocean on US winter precipitation variability. The tripolar height spatial pattern itself hints toward its origin in the eastern Indian Ocean.

A close examination of the errors in NMME predicted Indian Ocean SST reveals that notwithstanding the cold bias in most regions, the predicted SST difference between two winters is closer to the observation in the Southwest Indian Ocean, where the local SST pattern may be in the most predictable mode resulting from ENSO-induced thermocline variation (Wu & Tang, 2019). It is noted that although the influence of Indian Ocean SST variability may be smaller than that of ENSO-related SST variability (e.g., Hu et al., 2023), a small modulation in the atmospheric response by the former, nonetheless, can be important for bringing incremental improvements in seasonal prediction skill.

The present study focuses on the analysis of 2021 and 2022 La Niña years and does not include the analysis of the more recent 2023 La Niña. The former two cold events had a similar intensity over the entire boreal winter season (November–March), but the intensity of the latter event was much weaker (https://origin.cpc.ncep.noaa.gov/products/analysis_monitoring/ensostuff/ONI_v5.php). Further studies are needed to explore the relative importance of Indian Ocean SST including the role of SST warming trend and ENSO SST to the difference in the response of atmospheric teleconnections among the three consecutive La Niña events.

Data Availability Statement

The observed SST, precipitation and geopotential height data are available from the website of the NOAA Physical Sciences Laboratory at https://psl.noaa.gov/data/. The NMME model data used in this work are available from the website of the International Research Institute for Climate and Society's Data Library at https://

iridl.ldeo.columbia.edu/SOURCES/.Models/.NMME/. The large ensemble of FV3GFS AMIP simulations is publicly available at (Zhang et al., 2023) https://doi.org/10.5281/zenodo.8023560.

Acknowledgments
This work was supported by NOAA's Climate Program Office.

References

Annamalai, H., Okajima, H., & Watanabe, M. (2007). Possible impact of the Indian Ocean SST on the Northern Hemisphere circulation during El Niño. *Journal of Climate*, *20*(13), 3164–3189. https://doi.org/10.1175/JCLI4156.1

Bader, J., & Latif, M. (2005). North Atlantic Oscillation response to anomalous Indian Ocean SST in a coupled GCM. *Journal of Climate*, *18*(24), 5382–5389. https://doi.org/10.1175/JCLI3577.1

Beaudin, É., Di Lorenzo, E., Miller, A. J., Seo, H., & Joh, Y. (2023). Impact of extratropical Northeast Pacific SST on U.S. West Coast precipitation. *Geophysical Research Letters*, *50*(3), e2022GL102354. https://doi.org/10.1029/2022GL102354

Cao, T.-W., Zheng, F., & Fang, X.-H. (2022). Key processes on triggering the moderate 2020/21 La Niña event as depicted by the clustering approach. *Frontiers in Earth Science*, *10*, 822854. https://doi.org/10.3389/feart.2022.822854

Hoerling, M. P., Hurrell, J. W., Xu, T., Bates, G. T., & Phillips, A. S. (2004). Twentieth century North Atlantic climate change. Part II: Understanding the effect of Indian Ocean warming. *Climate Dynamics*, *23*(3–4), 391–405. https://doi.org/10.1007/s00382-004-0433-x

Hoerling, M. P., & Kumar, A. (2002). Atmospheric response patterns associated with tropical forcing. *Journal of Climate*, *15*(16), 2184–2203. https://doi.org/10.1175/1520-0442(2002)015<2184:arpawt>2.0.co;2

Hu, Z.-Z., Kumar, A., Jha, B., Chen, M., & Wang, W. (2023). The tropical Indian Ocean matters for U. S. winter precipitation variability and predictability. *Environmental Research Letters*, *18*(7), 074033. https://doi.org/10.1088/1748-9326/ace06e

Huffman, G. J., Adler, R. F., Arkin, P., Chang, A., Ferraro, R., Gruber, A., et al. (1997). The Global Precipitation Climatology Project (GPCP) combined precipitation dataset. *Bulletin of the American Meteorological Society*, *78*(1), 5–20. https://doi.org/10.1175/1520-0477(1997)078<0005:TGPCPG>2.0.CO;2

Hurrell, J., Hack, J., Shea, D., Caron, J., & Rosinski, J. (2008). A new sea surface temperature and sea ice boundary dataset for the Community Atmosphere Model. *Journal of Climate*, *21*(19), 5145–5153. https://doi.org/10.1175/2008JCLI2292.1

Kalnay, E., Kanamitsu, M., Kistler, R., Collins, W., Deaven, D., Gandin, L., et al. (1996). The NCEP NCAR 40-year reanalysis project. *Bulletin of the American Meteorological Society*, *77*(3), 437–472. https://doi.org/10.1175/1520-0477(1996)077<0437:TNYRP>2.0.CO;2

Kirtman, B. P., Min, D., Infanti, J. M., Kinter, J. L., Paolino, D. A., Zhang, Q., et al. (2014). The North American multimodel ensemble: Phase-1 seasonal-to-interannual prediction; phase-2 toward developing intraseasonal prediction. *Bulletin of the American Meteorological Society*, *95*(4), 585–601. https://doi.org/10.1175/bams-d-12-00050.1

Kumar, A., Chen, M., Hoerling, M. P., & Eischeid, J. (2013). Do extreme climate events require extreme forcings? *Geophysical Research Letters*, *40*(13), 3440–3445. https://doi.org/10.1002/grl.50657

Kumar, A., & Hoerling, M. P. (1995). Prospects and limitations of seasonal atmospheric GCM predictions. *Bulletin of the American Meteorological Society*, *76*(3), 335–345. https://doi.org/10.1175/1520-0477(1995)076%3c0335:PALOSA%3e2.0.CO;2

Kumar, A., Jha, B., & L'Heureux, M.-L. (2010). Are tropical SST trends changing the global teleconnection during La Niña? *Geophysical Research Letters*, *37*(12), L12702. https://doi.org/10.1029/2010GL043394

Li, X., Hu, Z.-Z., McPhaden, M. J., Zhu, C., & Liu, Y. (2023). Triple-Dip La Niñas in 1998–2001 and 2020–2023: Impact of mean state changes. *Journal of Geophysical Research: Atmospheres*, *128*(17), e2023JD038843. https://doi.org/10.1029/2023JD038843

Li, X., Hu, Z.-Z., Tseng, Y.-h., Liu, Y., & Liang, P. (2022). A historical perspective of the La Niña Event in 2020/21. *Journal of Geophysical Research: Atmospheres*, *127*(7), e2021JD035546. https://doi.org/10.1029/2021JD035546

Nishihira, G., & Sugimoto, S. (2022). Severe cold winters in East Asia linked to first winter of La Niña events and in North America linked to second winter. *Geophysical Research Letters*, *49*(7), e2021GL095334. https://doi.org/10.1029/2021GL095334

Okumura, Y. M., DiNezio, P., & Deser, C. (2017). Evolving impacts of multiyear LaNiña events on atmospheric circulation and U.S. drought. *Geophysical Research Letters*, *44*(22), 11614–11623. https://doi.org/10.1002/2017GL075034

Wu, Y., & Tang, Y. (2019). Seasonal predictability of the tropical Indian Ocean SST in the North American multimodel ensemble. *Climate Dynamics*, *53*(5–6), 3361–3372. https://doi.org/10.1007/s00382-019-04709-0

Zhang, T., Perlwitz, J., & Hoerling, M. P. (2014). What is responsible for the strong observed asymmetry in teleconnections between El Niño and La Niña? *Geophysical Research Letters*, *41*(3), 1019–1025. https://doi.org/10.1002/2013GL058964

Zhang, T., Yang, W., Quan, X., Zhu, J., Jha, B., Kumar, A., et al. (2023). A new GFSv15 based climate model large ensemble and its application to understanding climate variability, and predictability [Dataset]. Zenodo. https://doi.org/10.5281/zenodo.8023560

Zhou, L., Lin, S.-J., Chen, J.-H., Harris, L. M., Chen, X., & Rees, S. L. (2019). Toward convective-scale prediction within the next generation global prediction system. *Bulletin of the American Meteorological Society*, *100*(7), 1225–1243. https://doi.org/10.1175/bams-d-17-0246.1